

Bayesian Estimation of Gaussian Graphical Models with Projection Predictive Selection

Donald R. Williams¹, Juho Piironen², Aki Vehtari², and Philippe Rast¹

¹*Department of Psychology, University of California, Davis, USA*

²*Department of Computer Science, Aalto University, Espoo, Finland*

Abstract: Gaussian graphical models are used for determining conditional relationships between variables. This is accomplished by identifying off-diagonal elements in the inverse-covariance matrix that are non-zero. When the ratio of variables (p) to observations (n) approaches one, the maximum likelihood estimator of the covariance matrix becomes unstable and requires shrinkage estimation. Whereas several classical (frequentist) methods have been introduced to address this issue, Bayesian methods remain relatively uncommon in practice and methodological literatures. Here we introduce a Bayesian method for estimating sparse matrices, in which conditional relationships are determined with projection predictive selection. This method uses Kullback-Leibler divergence and cross-validation for variable selection, in addition to the horseshoe prior for regularization. Through simulation and an applied example, we demonstrate that the proposed method often outperforms both classical and alternative Bayesian estimators with respect to frequentist risk and consistently made the fewest false positives. We end by discussing limitations and future directions, as well as contributions to the Bayesian literature on the topic of sparsity.

Keywords and phrases: Bayesian, Gaussian Graphical Model, Projection Predictive Selection, Partial Correlation, Horseshoe Prior, Sparsity.

1. Introduction

Gaussian graphical models (GGM) are used for *covariance selection*, in which conditional dependencies between random variables are characterized (Dempster, 1972; Peng et al., 2009). This is accomplished by identifying off-diagonal elements in the inverse-covariance matrix (i.e., precision matrix) that are non-zero. When these covariances are standardized and the sign reversed, they correspond to partial correlations. Assuming multivariate normality, partial correlations imply pairwise conditional dependencies (i.e., direct effects) while controlling for all other variables included in the model (Baba et al., 2004; Baba and Sibuya, 2005). In contrast, marginal correlations consist of both direct and indirect relationships and this limits their use in assessing unique relationships among variables (Schäfer and Strimmer, 2005a). That *covariance selection* assesses conditional relationships has led to an extensive literature in both methodological and applied contexts. For example, GGMs are commonly used to characterize genetic regulatory networks (Wang, 2016), connectivity between brain regions (Das et al., 2017), and more recently to understand chronic mental illnesses (McNally et al., 2015).

The partial correlation matrix $\tilde{\mathbf{P}} = (\tilde{\rho}_{ij})$ can be obtained by inverting the corresponding covariance matrix Σ (Schäfer and Strimmer, 2005b). With each covariance $\hat{\omega}_{ij}$ (row

i and column j) and variances $\hat{\omega}_{ii}$ and $\hat{\omega}_{jj}$ the estimator follows

$$\tilde{r}_{ij} = \hat{\rho}_{ij} = \frac{-\hat{\omega}_{ij}}{\sqrt{\hat{\omega}_{ii}\hat{\omega}_{jj}}}, \text{ where } \hat{\Omega} = \begin{bmatrix} \hat{\omega}_{ii} & & \\ \vdots & \ddots & \\ \hat{\omega}_{ij} & \cdots & \hat{\omega}_{jj} \end{bmatrix} = \hat{\Sigma}^{-1}. \quad (1.1)$$

While this appears straightforward, equation 1.1 indicates that \tilde{r}_{ij} is a function of inverting the estimated $\hat{\Sigma}$. Typically, $\hat{\Sigma}$ is estimated via maximum likelihood (ML) but this approach yields reliable estimates only under ideal conditions (Won et al., 2009; Ledoit and Wolf, 2004). For example, Kuismin and Sillanpää (2016) demonstrated that ML-estimators of the eigenvalues can be non-optimal which then produce unstable estimates of $\hat{\omega}_{ij}$. When samples are small or the ratio of covariates p to observations n (p/n) is large (Wong et al., 2003), the estimated precision matrix $\hat{\Omega}$ may have inflated false-positives and/or false-negatives rates (Das et al., 2017). An additional limitation of ML-estimation is that the matrix will often suggest conditional dependencies between all variables ($\tilde{r}_{ij} \neq 0$); that is, $\hat{\Omega}$ does not typically contain elements equal to zero (Kuismin and Sillanpää, 2016). Furthermore, in high dimensional ($p > n$) settings, the ML-estimate cannot be computed due to singularity (Hartlap et al., 2007).

To address issues arising from estimating $\hat{\Sigma}$, at least two approaches have been proposed in the literature. One focuses on methods (e.g. shrinkage estimators) to improve parameter estimation (Huang and Wand, 2013; Kubokawa and Srivastava, 2008; Schäfer and Strimmer, 2005a), while the other generally focuses on sparse estimators that are commonly used to characterize GGMs (Wang, 2012; Yuan and Wang, 2013). For the present paper, we are interested in both sparsity and precise estimation. As such we present a method to accurately estimate the non-zero elements when the number of conditional relationships is small, that is, when most variables are conditionally independent ($\tilde{r}_{ij} = 0$).

In the classical literature (i.e., frequentist) there are two methods for sparse estimation, both of which rely on regularization techniques (Krämer et al., 2009; Ledoit and Wolf, 2004; Schäfer and Strimmer, 2005a). The first penalizes Ω such as the customary graphical LASSO (GLASSO) method (Friedman et al., 2008). The second approach uses penalized multiple regression and typically estimates \tilde{P} . In this approach, the input $n \times p$ matrix is standardized and each covariate p is regressed against the remaining $p - 1$ covariates. The partial correlation then follows

$$\hat{r}_{ij} = \text{sign}(\hat{\beta}_i^{(j)}) \sqrt{\hat{\beta}_i^{(j)} \hat{\beta}_j^{(i)}}, \quad (1.2)$$

where $\hat{\beta}_i^{(j)}$ is the penalized coefficient for predictor X_j and response X_i . Several regression approaches, including ridge (Van Wieringen and Peeters, 2016), partial least squares (Tenenhaus et al., 2008), and LASSO (Meinshausen and Bühlmann, 2006), have been used in this context. However, all except the LASSO (or variants such as the adaptive LASSO or Elastic net) require a decision rule to achieve sparsity. For this reason, the LASSO and related methods are popular in the GGM literature.

Although relatively uncommon, there are several Bayesian approaches for estimating Ω . These methods typically rely on the decomposition and regularization of the precision

matrix. For example, taking advantage of computational efficiency due to conjugacy, Wishart prior distributions on Ω have been investigated (Mohammadi and Wit, 2015b; Kuismi and Sillanpää, 2016). Bayesian LASSO has also been applied to Ω (Wang, 2012; Khondker et al., 2013) and for estimating \tilde{P} with the regression approach (Li and Zhang, 2017). These Bayesian estimators have compared favorably to classical methods (Khondker et al., 2013; Talluri et al., 2014); however, none (including classical methods) have proven optimal for sparse matrices (Kuismi and Sillanpää, 2016). Furthermore, since Bayesian approaches provide a measure of parameter uncertainty via the posterior distribution, parameters are never actually zero and variable selection must be achieved with a user-defined decision rule—this remains an active area of research (van der Pas et al., 2016). In the context of GGMs, Bayesian decision rules for *sparsifying* $\hat{\Omega}$ have included information criteria (Kuismi and Sillanpää, 2016), credible interval (varying widths) inclusion of zero (Khondker et al., 2013), and posterior model probabilities (Banerjee and Ghosal, 2013; Mohammadi and Wit, 2015a).

In the present paper, we introduce a novel Bayesian method for *covariance selection* that uses the regression approach to estimate \tilde{P} . To achieve sparsity, we use projection predictive selection, described in more detail in Section 3, that allows for variable exclusion ($\hat{\beta}_i^{(j)} = 0$) based on predictive utility (Goutis, 1998; Dupuis and Robert, 2003). This approach has been shown to outperform information criteria, cross-validation scores, or selecting the most probable variables (Piironen and Vehtari, 2017a). For regularization, we use the horseshoe prior which has desirable properties in high-dimensional settings (Carvalho et al., 2010; Piironen and Vehtari, 2017b). For example, hyperparameters on the shrinkage factors allow for large coefficients (i.e., strong signals) to incur minimal penalization (Piironen and Vehtari, 2017a).

The structure of this paper is as follows. In section 2, we introduce GGMs and the notation that will be used in the remainder of the paper and in section 3 we then discuss the projection predictive method and horseshoe prior in the context of GGM estimation. In section 4, we use numerical experiments to evaluate our methods performance compared to the LASSO regression approach described in (Krämer et al., 2009), the GLASSO method (Friedman et al., 2008), as well as a Bayesian method that utilizes a Wishart prior distribution and posterior probabilities for determining non-zero elements (Mohammadi and Wit, 2015b). In section 6, we apply projection predictive selection to a known genetic regulatory network. We end by addressing broader implications, limitations of the proposed method, and future directions.

2. Gaussian Graphical Models

Depending on the field, undirected graphical models refer to covariance selection models and random Markov fields. Here we adopted the term Gaussian graphical model, because it is common in the Bayesian literature and provides an informative description of the method. For example, consider a p -dimensional random variable X that follows a multivariate normal distribution

$$X = \{X_1, \dots, X_p\} \sim \mathcal{N}(\mu, \Sigma), \quad (2.1)$$

where, without loss of generality, we assume all variables have been standardized to have mean zero and variance one:

$$0 = \{\mu_1, \dots, \mu_p\}^\top, \text{ and } (\Sigma_{ii}) = 1. \quad (2.2)$$

Expanding this to multiple observations, X represents the data matrix of dimensions $n \times p$, with n observations. Following common notation, the graph is then denoted by $\mathcal{G} = (V, E)$ and consists of nodes $V = \{1, \dots, p\}$ as well as the edge set (non-zero connections between nodes) $E \subset V \times V$. The maximum edges possible in \mathcal{G} is $V(V-1)/2$, which correspond to the unique elements in Ω . Thus, while V represents the total number of columns in X , each dimension of Equation 2.1 is denoted by X_i . The edge set for \mathcal{G} contains nodes (X_i, X_j) that share a conditional relationship $X_i \perp\!\!\!\perp X_j | X_{V \setminus \{i, j\}}$. In contrast, conditionally independent nodes $X_i \perp\!\!\!\perp X_j | X_{V \setminus \{i, j\}}$ are not included in E and correspond to the zero elements within Ω .

Since we estimate \tilde{P} with the node wise (a.k.a., neighborhood selection) regression approach, our proposed method follows regression notation. This technique considers p regression models $\{1, \dots, p\}$, where one node is regressed against the remaining nodes

$$X_i = \sum_{j \neq i} \beta_j^{(i)} X_j + \varepsilon_i, \quad \varepsilon_i \sim \mathcal{N}(0, \sigma^2), \quad \{i = 1, \dots, p\}. \quad (2.3)$$

The regression coefficients and error variance then have a direct correspondence to $\tilde{\Omega}$

$$\beta_j^{(i)} = -\omega_{ij}/\omega_{ii} \text{ and } \sigma^2 = 1/\omega_{ii} \quad \{i = 1, \dots, p\}, \quad (2.4)$$

where ω_{ij} and ω_{ii} denote the off-diagonal and diagonal elements. The partial correlation matrix \tilde{P} , containing (\hat{r}_{ij}) , is obtained with Equation 1.2. These estimates are equivalent to standardizing the covariances of Ω and reversing the sign. For a pair of nodes, there are two approaches where $(X_i, X_j) \in E$. The first uses the “and” rule $\beta_i^j \neq 0$ and $\beta_j^i \neq 0$ whereas the second uses the “or” rule $\beta_i^j \neq 0$ or $\beta_j^i \neq 0$. Thus, from the p regression models, a $p \times p$ matrix is obtained that corresponds to the underlying structure of \mathcal{G} .

3. Projection Predictive Selection

Projective model selection is a model simplification technique and fundamentally a two-step procedure that provides a decision theoretically correct inference after selection. That is, the full posterior is projected to the restricted subspace instead of forming the usual posterior given constraints. First, for each node X_i $\{i = 1, \dots, p\}$ defined as the outcome variable y , we construct an encompassing reference model M_*

$$y = X\beta + \varepsilon, \quad \varepsilon \sim \mathcal{N}(0, \sigma^2), \quad (3.1)$$

that is regressed on a matrix X including the remaining nodes $(p-1)$. This model best captures our assumptions and uncertainties related to the problem, including the prior distributions. To obtain regularized estimates, our proposed method uses the horseshoe

prior

$$\begin{aligned}\beta_j | \lambda_j, \tau &\sim \mathcal{N}(0, \lambda_j^2 \tau^2) \quad \{j \neq i; j = 1, \dots, p\}, \\ \lambda_j &\sim \text{C}^+(0, 1), \\ \tau &\sim \text{C}^+(0, \tau_0),\end{aligned}\tag{3.2}$$

where C^+ is a half-Cauchy distribution for the local and global hyperparameters denoted with λ and τ , respectively. Following [Piironen and Vehtari \(2017b\)](#), the scale for τ can be selected to reflect ones prior belief about the number of expected edges p_0 for y

$$\tau_0 = \frac{p_0}{D - p_0} \frac{\sigma}{\sqrt{N}},\tag{3.3}$$

where D is the number of predictors ($p - 1$) in Equation 3.1.

In the second stage, for the p regression models, projective selection then determines which nodes can be removed, or set to zero ($\hat{\beta}_i^{(j)} = 0$), without introducing considerable predictive loss compared to the original reference model M_* . In the predictive framework, the model parameters of the reduced models – herein referred to as submodels including nodes x – are determined so that the resulting predictive distribution remains close to that of M_* ([Vehtari and Ojanen, 2012](#)). A theoretically justified and computationally convenient way to do this is by minimizing the discrepancy between the predictive distributions conditional on the parameter values, where the discrepancy δ is defined in terms of Kullback-Leibler (KL) divergence averaged over the empirical distribution for X ([Goutis, 1998](#); [Dupuis and Robert, 2003](#))

$$\begin{aligned}\theta_{\perp} &= \arg \min_{\theta' \in \Theta_{\perp}} \delta(\theta, \theta') \\ &\triangleq \arg \min_{\theta' \in \Theta_{\perp}} \frac{1}{n} \sum_{i=1}^n \text{KL}(p(\tilde{y} | \theta, X_i, M_*) \| p(\tilde{y} | \theta', x_i, M_{\perp})).\end{aligned}\tag{3.4}$$

This defines a parameter mapping $\Theta \mapsto \Theta_{\perp}$ where $\theta \in \Theta$ denotes the parameters of the reference model and $\theta_{\perp} \in \Theta_{\perp}$ the parameters of the projected submodel M_{\perp} . Given a set of posterior draws $\{\theta_s\}_{s=1}^S$ for the reference model, we can then project these individually according to Equation (3.4) to obtain the projected posterior draws $\{\theta_{\perp}^s\}_{s=1}^S$ for any submodel M_{\perp} . It can be shown that the projected regression coefficients are obtained analytically by the least squares solution where the target values are replaced by the fit of the reference model for a particular posterior draw (see the appendix of [Piironen and Vehtari, 2017a](#)). The projection loss is then defined as the mean discrepancy over the posterior of the reference model

$$L = \frac{1}{S} \sum_{s=1}^S \delta(\theta_s, \theta_{\perp}^s).\tag{3.5}$$

We then seek a reduced model with minimal loss by using a forward search strategy, in which nodes are sequentially added that minimize δ . A direct consequence of defining

the model parameters of the submodels as projections of the reference model is that the prior is only specified for the reference model and this information is also then transmitted to the submodels in the projection.

To assess the accuracy of the reduced models in the second step, we use approximate leave-one-out (LOO) cross-validation with Pareto smoothed importance sampling (PSIS), which avoids the repeated fitting of the reference model, but requires the selection to be performed n times. In (PS)IS-LOO, the posterior draws can be treated as draws from the LOO posteriors after weighting them by the importance weights

$$w_{is} \propto \frac{1}{p(y_i | \theta_s)} \quad (3.6)$$

which are then smoothed to stabilize the LOO estimates (Vehtari et al., 2016). Thus the projection is carried out with the data point i left out, where the submodel draws $\{\theta_s\}_{s=1}^S$ are weighted with w_{is} when predicting the left-out point. This gives an estimate of the predictive accuracy \hat{u}_k with some standard error s_k for a given model complexity k (number of nodes, for instance). As an accuracy measure, we use log predictive density (LPD).

Our decision rule for achieving sparsity ($\hat{\beta}_i^{(j)} = 0$) is based on \hat{u}_k . We select the simplest model that has an acceptable difference $\Delta u > 0$ relative to the reference model \hat{u}_* with some level of confidence α . That is, we choose the simplest model satisfying

$$\Pr [u_* - u_k \leq \Delta u] \geq 1 - \alpha, \quad (3.7)$$

which is estimated using the Bayesian bootstrap. The choices for Δu and α are made on subjective grounds depending on how much one is willing to sacrifice predictive accuracy for making the model simpler. In other words, sparsifying \mathcal{G} can be viewed as a trade-off between node-wise predictive loss and parsimony. A reasonable but generic choice for Δu would be 5 or 10 percent of the difference $\hat{u}_* - \hat{u}_0$, where \hat{u}_0 denotes the accuracy estimate for the simplest possible (null) model (Piironen and Vehtari, 2017a).

From each node-wise regression, the coefficients and zero-entries are placed into a $p \times p$ matrix $\Lambda_{i,i \neq i}$. Following Equation 1.2, but applied to the the entire matrix, we calculate the partial correlations as

$$\tilde{\mathbf{P}} = \text{sign}(\Lambda) \sqrt{\Lambda \Lambda^\top}, \quad (3.8)$$

where both $\beta_i^j \neq 0$ and $\beta_j^i \neq 0$ must be non-zero for inclusion in the edge set E of the graph \mathcal{G} . While this procedure is not computationally cheap, each regression is estimated once and prior information (e.g., theoretical considerations) regarding node specific sparsity can be included by setting τ_0 in Equation 3.2.

Algorithm 1 GGM: Projection Predictive Selection

1. For each node X_i $\{i = 1, \dots, p\}$ fit a reference model M_{*i} (Equation 3.1)
2. For M_{*i} :
 - (a) Forward variable search based on minimizing loss according to KL-divergence (Equations 3.4 – 3.5)

- (b) Compute predictive accuracy \hat{u}_k with approximate LOO and Pareto smoothed importance weights w_{is} , where k is the model size (Equation 3.6)
- (c) Select simplest model with acceptable predictive difference from the reference model (Equation 3.7)
 - i. Set parameter estimates for excluded variables to zero ($\beta_i^j = 0$)
- (d) Place non-zero ($\beta_i^j \neq 0$) and zero estimates ($\beta_i^j = 0$) into a $p \times p$ matrix $\Lambda_{i,i \neq i}$

3. When $i = p$, compute the partial correlation matrix $\tilde{\mathbf{P}}$ from Λ (Equation 3.8)

4. Simulation Study

We performed extensive simulations to characterize the performance of our proposed method compared to three alternatives:

- A Bayesian approach that uses a novel birth-death MCMC algorithm BDMCMC. While only characterized in one paper, BDMCMC often outperformed more common approaches (e.g., GLASSO) in terms of identifying *true* edges and KL-divergence (R package: *BDgraph*).
- The Graphical lasso (GLASSO) method that is considered a state-of-art approach for estimating Ω . Following (Kuismi and Sillanpää, 2016), we chose the tuning parameter ρ with the extended Bayesian information criterion (EBIC). The tuning parameter γ for EBIC was set to 0.5 (R package: *glasso*).
- A node-wise regression approach that uses LASSO regularization to estimate the partial correlation matrix. Following Krämer et al. (2009), the tuning parameter was selected with k-fold cross-validation (R package: *parcor*).

We also included an additional projection predictive estimator (PROJ-Wkly), but with a *weakly* informative prior defined as $\beta \sim \mathcal{N}(0, 5)$. This allowed for determining whether the horseshoe prior (PROJ-HS) is necessary for good performance. For the simulation, we chose generic values for $\tau_0 = 1$ (Equation 3.2), $\Delta u = 10\%$ (Equation 3.7), and $\alpha = 90\%$ (Equation 3.7). This choice of τ_0 follows common practice (Piironen and Vehtari, 2017a), whereas the values for Δu and α were shown to be reasonable choices for variable selection. Each model consisted of two chains of 1,500 samples each (excluding 1,500 warm-up iterations), and were fitted with the R package *bnets* (github: *bnets*) that serves as a front end to *Stan* (Stan Development Team, 2016). For predictive selection in particular, *bnets* uses *rstanarm* (Gabry and Goodrich, 2016) for model fitting and *projpred* for the projection (Paasiniemi et al., 2017). All computations were done in R version 3.4.2 (R Core Team, 2016).

We examined performance across three structured and three unstructured graphs (Figure 1):

1. *AR(1)*: A matrix with $\sigma_{ii'} = 0.7^{|k-k'|}$.
2. *AR(2)*: A matrix with $\theta_{kk} = 1$, $\theta_{kk-1} = \theta_{k-1k} = 0.5$, and $\theta_{kk-2} = \theta_{k-2k} = 0.5$.
3. *Cluster*: A matrix consisting of clusters, each of which has a randomly structured edge set E . The number maximum number of clusters is $\max\{2, [p/20]\}$.

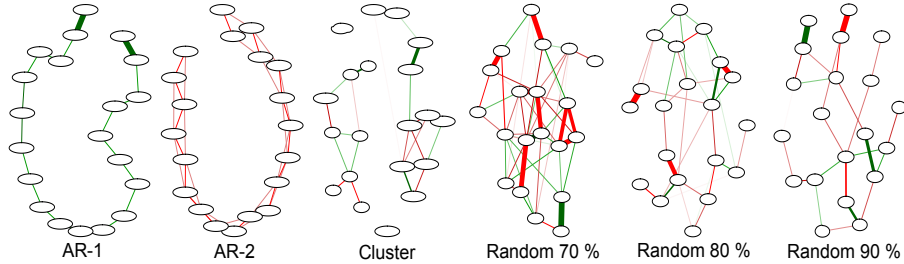


Fig 1: Example graph structures

4. *Random*: 70 % of the off-diagonal elements set to zero.
5. *Random*: 80 % of the off-diagonal elements set to zero.
6. *Random*: 90 % of the off-diagonal elements set to zero.

For the cluster and unstructured graphs, the edge set E was randomly generated from a Bernoulli distribution and the corresponding matrix from $\Omega \sim W_G(3, I_p)$. The number of nodes p was fixed to 20 and the sample sizes n varied (10, 20, 40, 80, 100, and 200). When preparing the simulations, we noticed that performance can depend on the values within E , which are generally not controlled in graphical simulations. We therefore followed Krämer et al. (2009) and Schäfer and Strimmer (2005b), such that a new matrix was generated for each of the 50 iterations (per condition).

4.1. Performance measures

4.1.1. Loss Functions

We considered two loss functions, each of which allowed for quantifying the risk associated with the estimated graphs. For each estimator, the errors were computed for the estimated partial correlation matrix \hat{P} and included absolute differences (L_1) and squared differences (L_2) defined as

$$L_1 = \frac{1}{n} \sum_{i=1}^n |P_i - \hat{P}_i| \text{ and } L_2 = \frac{1}{n} \sum_{i=1}^n (P_i - \hat{P}_i)^2 \quad (4.1)$$

where the expectation was taken as the average across the n iterations ($i = 1, \dots, n$). Lower values indicated less discrepancy from the *true* generating matrix, such that the optimal estimator was closest to zero.

4.1.2. Sparsity

Because the trade-off between false-negatives and positives is research question specific, we considered three measures of performance. Sensitivity (SE) is the true positive rate

and specificity (SP) is the true negative rate ($1 - SP$ = false positive rate)

$$SE = \frac{TP}{TP + FN} \text{ and } SP = \frac{TN}{TN + FP}, \quad (4.2)$$

in which TP and FP are the true and false positives. The false negatives and true negatives are denoted FN and TN. A perfect score (i.e., 1) for specificity can be obtained without identifying any *true* edges, so we also computed $F1 -$ scores defined as

$$F1 - \text{score} = \frac{2TP}{2TP + FP + FN}, \quad (4.3)$$

where both precision (i.e., positive predictive value) and sensitivity are considered. This measure ranges from 0 – 1, with a perfect score as 1.

5. Results

5.1. Loss Functions

The results are presented in Figure 2. For each condition, the optimal estimator is denoted with a star. Most surprisingly, given its popularity, the GLASSO method provided the lowest error only twice. This finding is similar to [Kuismin and Sillanpää \(2016\)](#), where GLASSO also did not compare favorably to the other methods under consideration. The present result also confirms [Mohammadi and Wit \(2015a\)](#), where the BDMCMC method regularly outperformed classical regression approaches and the GLASSO with respect to KL-divergence. While all methods were consistent, such that error reduced with increasing sample sizes, it is clear that the Bayesian methods collectively provided far superior performance than the classical methods. This is particularly interesting, because these outcomes evaluated the frequentist properties of Bayesian models.

The projection predictive approach compared favorably to the other methods, especially the LASSO and GLASSO methods. The PROJ-HS approach also had the best performance in many conditions. This was particularly the case for the structured graphs and L_1 loss. Indeed, for L_1 error, PROJ-HS had the best performance in 17 out of 36 conditions in total. In contrast, for L_2 error, the BDMCMC method had the best overall performance (25 out of 36). These results demonstrate the utility of the horseshoe prior (PROJ-HS) for improved parameter estimation. For example, the errors were generally lower than when a weakly informative prior distribution was used.

5.2. Sparsity

The results are presented in Figure 3. For each condition, the optimal estimator is denoted with a star. The GLASSO method had similar performance as the risk estimates (Figure 3); for example, it provided the best estimate in only 3 out of 108 conditions. With respect to $F1$ -scores, the present results are similar to [Mohammadi and Wit \(2015a\)](#) where the BDMCMC method often had superior performance. However, for $p > n$ scenarios in particular, the BDMCMC method also had the lowest specificity which indicates the estimated graphs were too dense. Specifically, for three conditions, the false positive

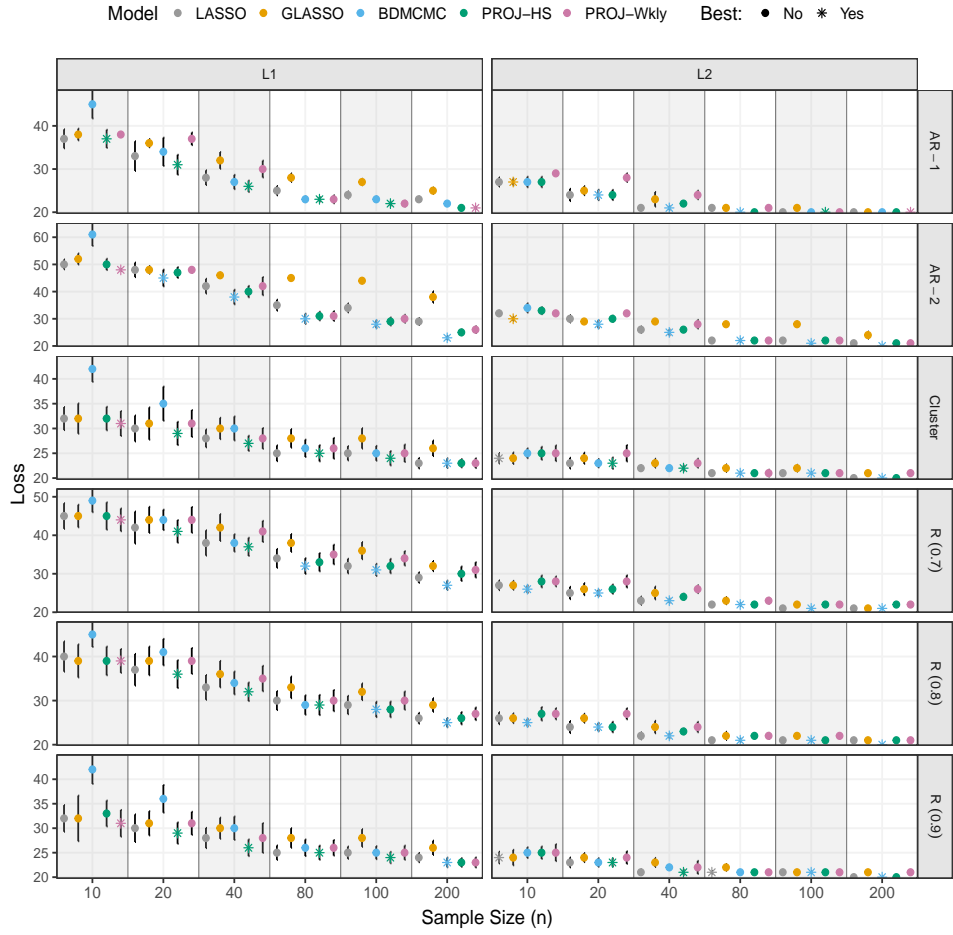


Fig 2: Risk estimates (R = Random). LASSO regression (LASSO), graphical LASSO (GLASSO), birth-death MCMC (BDMCMC), projection with a horseshoe prior (PROJ-HS), and projection with a weakly informative prior (PROJ-Wkly). The optimal estimator is denoted with a star (*).

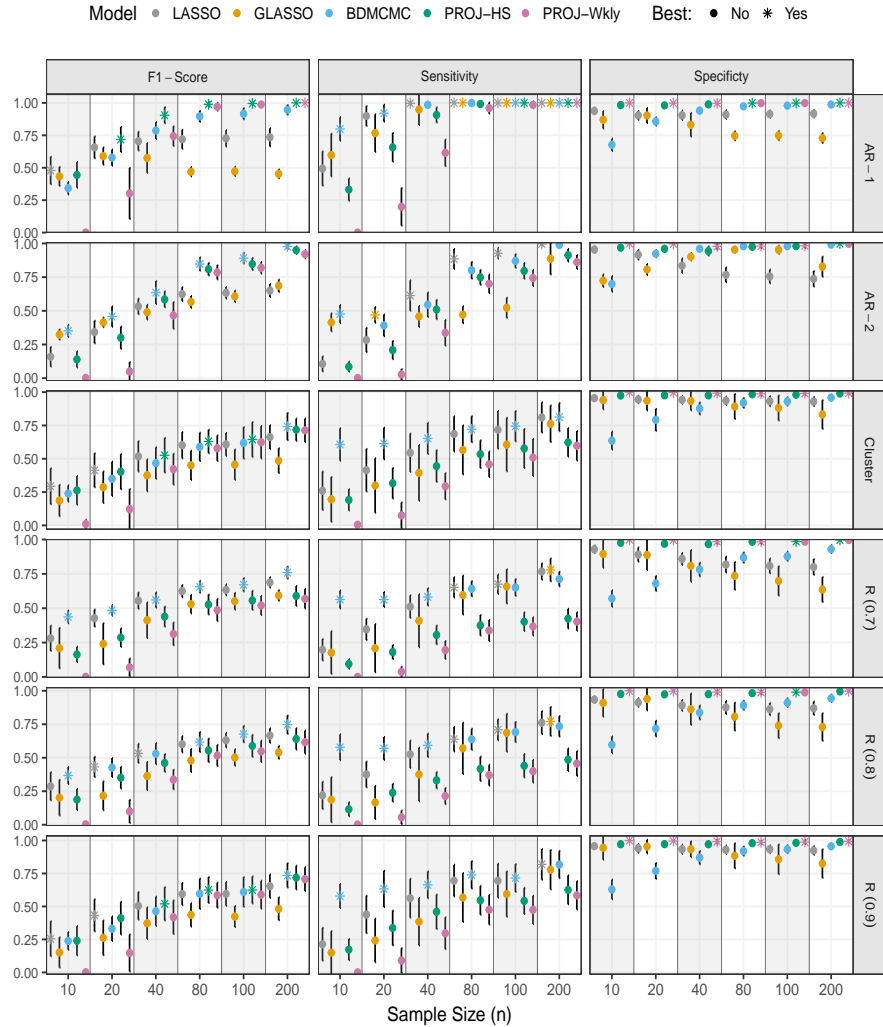


Fig 3: Edge identification (R = Random). LASSO regression (LASSO), graphical LASSO (GLASSO), birth-death MCMC (BDMCMC), projection with a horseshoe prior (PROJ-HS), and projection with a weakly informative prior (PROJ-Wkly). The optimal estimator is denoted with a star (*).

rate exceeded 30 % (1 - specificity). With large samples sizes, specificity ultimately increased and was comparable to other methods when $p/n < 1$.

The proposed method had some desirable qualities, but also some potential limitations. First, for the F1-scores, PROJ-HS provided the highest estimate in 11 out of 36 conditions. In contrast, PROJ-Wkly generally had a lower F1-scores and this further highlights the utility of the horseshoe prior. Furthermore, the discrepancy between priors distribution was most pronounced in high dimensional settings, as PROJ-Wkly often had the lowest possible F1-score of 0. In comparison to the GLASSO method, PROJ-HS had higher F1-scores for 31 out of 36 conditions. This suggest our proposed method offers clear advantages when compared to one of the more popular and well-characterized methods for estimating sparse graphs.

The results for sensitivity highlight some potential limitations of our proposed method. The projective method consistently had the lowest sensitivity and, in fact, this was the case for all conditions. While this pattern was observed for both prior distributions, PROJ-HS regularly detected more *true* edges than PROJ-Wkly. Importantly, although sensitivity was relatively low, the PROJ methods also had the highest specificity. In fact, for all simulation conditions the PROJ methods combined to make the fewest false positives. This result was striking, because it did not depend on the sample size, p/n ratio, or graphical structure.

Additionally, we observed some surprising patterns for the LASSO and GLASSO methods: for several of the graphical structures, specificity decreased with larger sample sizes. In other words, contrary to what one might expect, false positives increased with more observations. This also illustrates important difference between regression approaches (PROJ vs LASSO). That is, the projective method produced fewer false positives than the LASSO method, even though LASSO does not require an explicit decision rule for achieving sparsity.

For specificity, there were differences between prior distributions in that the weakly informative prior consistently had the higher score. This may be partly related to PROJ-Wkly also identifying fewer *true* edges than PROJ-HS, although we cannot be entirely sure. It should be noted that difference between methods were often within 1 % so may reflect sampling variability due to relatively few iterations per condition (50). Nonetheless, when taking both sensitivity and specificity into account, PROJ-HS appears to offer a reasonable compromise that does not depend on the simulation condition (at least for making false positive).

6. Application

6.1. Sachs Protein-Signaling Network

We now compare methods on the *so-called* Sach's network ($p = 11$ and $n = 7466$). These data were first characterized in [Sachs et al. \(2005\)](#), where they used Bayesian methods to suggest causal protein-signaling between phosphorylated proteins and phospholipids. The identified edges (connection between nodes) were then confirmed with experimental manipulations. Because this network is known, it has been used extensively to evaluate the performance of novel GGM methods or decision rules for existing methods. For

example, these data (located in the R package *gss*) have been analyzed with the GLASSO method (Friedman et al., 2008), Bayesian LASSO covariance penalization (Khondker et al., 2013), maximum a posteriori estimation (MAP) (Kuismin and Sillanpää, 2017), and the Ledoit and Wolf estimator (Kuismin and Sillanpää, 2017).

To allow for comparison beyond the methods in this paper, we computed two additional measures of classification accuracy. Matthews correlation coefficient is defined as

$$MCC = \frac{TP \times TN - FP \times FN}{\sqrt{(TP + FP)(TP + FN)(TN + FP)(TN + FN)}}, \quad (6.1)$$

where the value can range between -1 and 1. The second additional measure is precision, or the positive predictive value

$$PPV = \frac{TP}{TP + FP}. \quad (6.2)$$

The results are displayed visually in Figure 4 and reported in Table 1. There were clear differences between projection selection and the other methods; most notably, LASSO, GLASSO, and BDMCMC all estimated very dense graphs in which specificity did not exceed 0.30 (false positive rate > 0.70). In fact, the LASSO method estimated a fully connected graphical structure. In contrast, the projection selection had much higher specificity, while sensitivity was lower than the other methods. In this example, due to the large sample size, different prior distributions produced similar estimates. In practice, a more informative prior can be implemented by setting τ_0 (Equation 3.2) to a lower value.

Each method has flexibility in model specification, which can possibly improve estimation. We explored this possibility with all three methods. For the LASSO, we set the fold number to 10 and 20, both of which provided the same result. Next, we explored several gamma γ parameters for EBIC model selection with GLASSO. With a large value ($\gamma = 50$) we were able to decrease the false positive rate from 0.78 to 0.53. These results may reflect that the LASSO solution approaches the maximum likelihood estimate when the sample size is large (Kuismin and Sillanpää, 2017).

For BDMCMC, we made two adjustments to the default settings: (1) for increased penalization (i.e., shrinkage), we increased the degrees of freedom parameter r of the Wishart prior distribution (default = 3); and (2) increased the cut-off for the posterior inclusion probability (PIP; default = 0.5). With $r = 100$, the false positive rate decreased by only 0.05 which suggests diminishing returns from the prior distribution in large sample settings. We then set the PIP cut-off to 0.99 and this further reduced the false positive rate from 0.72 to 0.58.

In comparison to the Bayesian literature, our proposed method achieved one of the highest scores for MCC, specificity, and precision to date (to our knowledge). In Kuismin and Sillanpää (2017), their proposed MAP estimator with EBIC had sensitivity of 0.63 and a false positive rate of 0.42. In Khondker et al. (2013), the covariance matrix was penalized with the Bayesian LASSO (Park and Casella, 2008) and varying credible interval widths were used for determining the edge set E . The highest precision ($PPV = 0.63$) was obtained with 50 % credible intervals, but at the cost of reduced sensitivity (0.26). Together, at least for these data, the projection method offers a clear

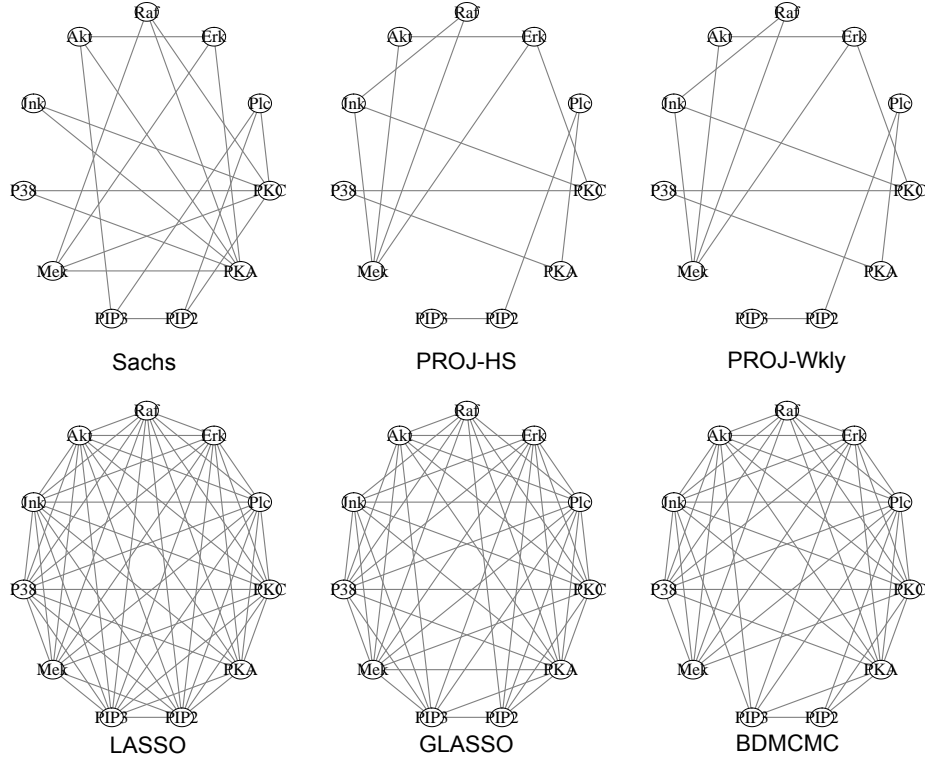


Fig 4: Sachs protein-signaling network: LASSO regression (LASSO), graphical LASSO (GLASSO), birth-death MCMC (BDMCMC), projection with a horseshoe prior (PROJ-HS), and projection with a weakly informative prior (PROJ-Wkly)

advantage with respect to not only limiting false positives but also maintaining sensitivity to detect *true* edges.

7. Conclusion

We introduced a Bayesian method for estimating Gaussian graphical models with projection predictive selection (Section 3). For determining zeros, or sparsifying the graph, the proposed method is framed in terms of tolerable predictive loss from a reference model. With numerical experiments, we demonstrated that this method often outperforms both classical and Bayesian methods, both in terms of frequentist risk measured with loss functions and identifying the *true* structure of a graph. For specificity (and thus false positives) in particular, projection selection consistently had the best performance and the scores were largely independent of the simulation condition. Furthermore, when applied to a known protein-signaling network, we showed that our approach not only

TABLE 1
Performance measures for identifying the Sachs network. LASSO regression (LASSO), graphical LASSO (GLASSO), birth-death MCMC (BDMCMC), projection with a horseshoe prior (PROJ-HS), projection with a weakly informative prior (PROJ-Wkly), Matthew's correlation coefficient (MCC), and the positive predictive value (PPV).

	LASSO	GLASSO	BDMCMC	PROJ-HS	PROJ-Wkly
F1-score	0.49	0.58	0.57	0.50	0.50
Sensitivity	0.95	1.00	0.95	0.42	0.42
Specificity	0.00	0.22	0.28	0.86	0.86
False Positive	1.00	0.78	0.72	0.14	0.14
MCC	-0.19	0.30	0.27	0.32	0.32
PPV	0.33	0.40	0.41	0.62	0.62

outperformed the alternative methods in this work, but also other approaches in the literature with respect to specificity and precision.

Despite these promising findings, none of the methods provided the best performance for all conditions or loss functions. In Section 6, for example, we actively pursued a sparse graph but discovery (minimizing false negatives) could be important to consider. We focused on specificity for two reasons: (1) based on the results, we attempted to outperform projection selection by adjusting the settings of the competing methods. This strengthened our conclusion that projection selection estimates the fewest false positives; and (2) the classical methods produced such dense graphs that it did not make sense (or was not possible for LASSO) to increase connectivity. Of course, while not explored here, the projection method readily allows for denser graphs by adjusting the decision rule for setting coefficients to zero (Section 3).

Furthermore, with respect to accurately estimating non-zero partial correlations, the projection method (PROJ-HS) often had the lowest L_1 error and BDMCMC consistently had the lowest L_2 error. As such, minimizing each loss function can guide which model is used in practice; for example, if penalizing larger errors is not desired, then the projection method should be adopted based on decision theoretic considerations (Robert, 2007). Importantly, the simulation results demonstrated that the Bayesian methods (projection selection and BDMCMC) offer clear advantages compared to classical methods, especially the GLASSO method with EBIC selection. This was surprising for two reasons: (1) due to the popularity of GLASSO; and (2) that GLASSO consistently provided poor performance for all outcomes (loss functions and edge identification), both with simulated (Section 5) and real data (6).

There are several important limitations. First, we selectively chose the comparison methods based on ease of implementation (R packages) (Kuismi and Sillanpää, 2017), popularity in various literatures (Epskamp and Fried, 2016), and what is typically used in simulations (Kuismi and Sillanpää, 2017; Mohammadi and Wit, 2015a). Therefore, our conclusions are restricted to these conditions, graphical structures, and decision rules. For example, in addition to EBIC selection, GLASSO can be used with the rotation information criterion, stability approach for regularization selection, and cross-validation. Second, the projection method is computationally greedy which makes it relatively slow, but not impractically so. The simulations were completed within 24 hours, and this readily allows for use in methodological as well as practical applications.

More generally, this work is important in the Bayesian literature. A central challenge

in Bayesian statistics is developing methods and decision rules for achieving sparsity (Piironen and Vehtari, 2017a; van der Pas et al., 2016), especially in high dimensional settings. For example, in contrast to the classical LASSO, the Bayesian LASSO requires an explicit decision rule for variable selection (Khondker et al., 2013). We demonstrated projection selection, a relatively uncommon approach, offers advantages compared to posterior probabilities (Mohammadi and Wit, 2015a), information criterion (Kuismi and Sillanpää, 2017) or credible interval exclusion of zero (Khondker et al., 2013). Furthermore, even in a large n setting (Section 6), where the data can overwhelm the prior, the projection method maintained high specificity and precision.

The proposed method can be extended in many ways; for example, to handle mixed graphical models (continuous and binary variables), longitudinal data, and non-normal data. Additionally, the projection can be carried out on the inverse-covariance matrix and alternative samplers can be implemented, each of which could possibly improve efficiency. We plan to explore these options in the future.

Acknowledgement

Research reported in this publication was supported by three funding sources: (1) The National Academies of Sciences, Engineering, and Medicine FORD foundation pre-doctoral fellowship to DRW; (2) The National Science Foundation Graduate Research Fellowship to DRW; and (3) the National Institute On Aging of the National Institutes of Health under Award Number R01AG050720 to PR. The content is solely the responsibility of the authors and does not necessarily represent the official views of the National Academies of Sciences, Engineering, and Medicine, the National Science Foundation, or the National Institutes of Health.

References

Baba, K., Shibata, R., and Sibuya, M. (2004). “Partial Correlation and Conditional Correlation as Measures of Conditional Independence.” *Australian & New Zealand Journal of Statistics*, 46(4): 657–664.
 URL <http://doi.wiley.com/10.1111/j.1467-842X.2004.00360.x> 1

Baba, K. and Sibuya, M. (2005). “Equivalence of Partial and Conditional Correlation Coefficients.” *J. Japan Statist. Soc.*, 35(1): 1–19. 1

Banerjee, S. and Ghosal, S. (2013). “Bayesian estimation of a sparse precision matrix.” *arXiv*.
 URL <http://arxiv.org/abs/1309.1754> 3

Carvalho, C. M., Polson, N. G., and Scott, J. G. (2010). “The horseshoe estimator for sparse signals.” *Biometrika*, 97(2): 465–480. 3

Das, A., Sampson, A., Lainscsek, C., Muller, L., Lin, W., Doyle, J., Cash, S., Halgren, E., and Sejnowski, T. (2017). “Interpretation of the Precision Matrix and Its Application in Estimating Sparse Brain Connectivity during Sleep Spindles from Human Electrocorticography Recordings.” *Neural computation*, 29(3): 603–642. 1, 2

Dempster, A. (1972). “Covariance Selection.” *Biometrics*, 28(1): 157–175.
 URL <http://www.jstor.org/stable/2528966?origin=crossref> 1

Dupuis, J. A. and Robert, C. P. (2003). “Variable selection in qualitative models via an entropic explanatory power.” *Journal of Statistical Planning and Inference*, 111(1-2): 77–94. 3, 5

Epskamp, S. and Fried, E. I. (2016). “A Tutorial on Regularized Partial Correlation Networks.” URL <http://arxiv.org/abs/1607.01367> 15

Friedman, J., Hastie, T., and Tibshirani, R. (2008). “Sparse inverse covariance estimation with the graphical lasso.” *Biostatistics*, 9(3): 432–441. URL <https://academic.oup.com/biostatistics/article-lookup/doi/10.1093/biostatistics/kxm045> 2, 3, 13

Gabry, J. and Goodrich, B. (2016). “rstanarm: Bayesian Applied Regression Modeling via Stan.” URL <https://cran.r-project.org/package=rstanarm> 7

Goutis, C. (1998). “Model choice in generalised linear models: a Bayesian approach via Kullback-Leibler projections.” *Biometrika*, 85(1): 29–37. URL <http://biomet.oupjournals.org/cgi/doi/10.1093/biomet/85.1.29> 3, 5

Hartlap, J., Simon, P., and Schneider, P. (2007). “Unbiased estimation of the inverse covariance matrix.” *a&a*, 464: 399–404. URL <https://www.aanda.org/articles/aa/pdf/2007/10/aa6170-06.pdf> 2

Huang, A. and Wand, M. P. (2013). “Simple marginally noninformative prior distributions for covariance matrices.” *Bayesian Analysis*, 8(2): 439–452. URL <http://projecteuclid.org/euclid.ba/1369407559> 2

Khondker, Z. S., Zhu, H., Chu, H., Lin, W., and Ibrahim, J. G. (2013). “The Bayesian Covariance Lasso.” *Statistics and its interface*, 6(2): 243–259. URL <http://www.ncbi.nlm.nih.gov/pubmed/24551316> 3, 13, 16

Krämer, N., Schäfer, J., and Boulesteix, A.-L. (2009). “Regularized estimation of large-scale gene association networks using graphical Gaussian models.” *BMC Bioinformatics*, 10(1): 384. URL <http://www.biomedcentral.com/1471-2105/10/384> 2, 3, 7, 8

Kubokawa, T. and Srivastava, M. S. (2008). “Estimation of the precision matrix of a singular Wishart distribution and its application in high-dimensional data.” *Journal of Multivariate Analysis*, 99(9): 1906–1928. 2

Kuismin, M. and Sillanpää, M. J. (2016). “Use of Wishart prior and simple extensions for sparse precision matrix estimation.” *PLoS ONE*, 11(2): e0148171. URL <http://www.ncbi.nlm.nih.gov/pmc/articles/PMC4734711/> 2, 3, 7, 9

Kuismin, M. O. and Sillanpää, M. J. (2017). “Estimation of covariance and precision matrix, network structure, and a view toward systems biology.” *Wiley Interdisciplinary Reviews: Computational Statistics*, 9(6): 1–13. 13, 15, 16

Ledoit, O. and Wolf, M. (2004). “A well-conditioned estimator for large-dimensional covariance matrices.” *Journal of Multivariate Analysis*, 88(2): 365–411. 2

Li, F.-q. and Zhang, X.-s. (2017). “Bayesian Lasso with neighborhood regression method for Gaussian graphical model.” *Acta Mathematicae Applicatae Sinica, English Series*, 33(2): 485–496.

URL <http://link.springer.com/10.1007/s10255-017-0676-z> 3

McNally, R. J., Robinaugh, D. J., Wu, G. W. Y., Wang, L., Deserno, M. K., and Borsboom, D. (2015). “Mental Disorders as Causal Systems.” *Clinical Psychological Science*, 3(6): 836–849.

URL <http://journals.sagepub.com/doi/10.1177/2167702614553230> 1

Meinshausen, N. and Bühlmann, P. (2006). “High-dimensional graphs and variable selection with the Lasso.” *Annals of Statistics*, 34(3): 1436–1462. 2

Mohammadi, A. and Wit, E. C. (2015a). “Bayesian structure learning in sparse Gaussian graphical models.” *Bayesian Analysis*, 10(1): 109–138. 3, 9, 15, 16

— (2015b). “BDgraph: An R Package for Bayesian Structure Learning in Graphical Models.” URL <http://arxiv.org/abs/1501.05108> 3

Paasiniemi, M., Piironen, J., Gabry, J., and Vehtari, A. (2017). “projpred (R package version 0.6.0).” URL <https://github.com/stan-dev/projpred> 7

Park, T. and Casella, G. (2008). “The Bayesian Lasso.” *Journal of the American Statistical Association*, 103(482): 681–686. 13

Peng, J., Wang, P., Zhou, N., and Zhu, J. (2009). “Partial Correlation Estimation by Joint Sparse Regression Models.” *Journal of the American Statistical Association*, 104(486): 735–746.

URL <http://arxiv.org/abs/0811.4463> 1

Piironen, J. and Vehtari, A. (2017a). “Comparison of Bayesian predictive methods for model selection.” *Statistics and Computing*, 27(3): 711–735. 3, 5, 6, 7, 16

— (2017b). “On the Hyperprior Choice for the Global Shrinkage Parameter in the Horseshoe Prior.” *Proceedings of the 20th International Conference on Artificial Intelligence and Statistics*, 54: 905–913.

URL <http://arxiv.org/abs/1610.05559> 3, 5

R Core Team (2016). “R: A Language and Environment for Statistical Computing.” URL <https://www.r-project.org/> 7

Robert, C. (2007). “The Bayesian choice: from decision-theoretic foundations to computational implementation.” 77 – 81. 15

Sachs, K., Perez, O., Pe’er, D., Lauffenburger, D. A., and Nolan, G. P. (2005). “Causal protein-signaling networks derived from multiparameter single-cell data.” *Science*, 308(5721): 523–529. 12

Schäfer, J. and Strimmer, K. (2005a). “A Shrinkage Approach to Large-Scale Covariance Matrix Estimation and Implications for Functional Genomics.” *Statistical Applications in Genetics and Molecular Biology*, 4(1).

URL <https://www.degruyter.com/view/j/sagmb.2005.4.issue-1/sagmb.2005.4.1.1175/sagmb.2005.4.1.1175.xml> 1, 2

— (2005b). “An empirical Bayes approach to inferring large-scale gene association networks.” *Bioinformatics*, 21(6): 754–764.

URL <https://www.aanda.org/articles/aa/pdf/2007/10/aa6170-06.pdf> 1, 8

Stan Development Team (2016). “Rstan: the R interface to Stan.” URL <http://mc-stan.org/> 7

Talluri, R., Baladandayuthapani, V., and Mallick, B. K. (2014). “Bayesian sparse

graphical models and their mixtures.” *Stat*, 3(1): 109–125.
 URL <http://www.ncbi.nlm.nih.gov/pubmed/24948842> 3

Tenenhaus, A., Guillemot, V., Gidrol, X., and Frouin, V. (2008). “Gene Association Networks from Microarray Data using a Regularized Estimation of Partial Correlation based on.” *IEEE Transactions on Computational Biology and Bioinformatics*, 7(2): 251–262. 2

van der Pas, S., Szabó, B., and van der Vaart, A. (2016). “Uncertainty quantification for the horseshoe.” (4): 1221–1274.
 URL <http://arxiv.org/abs/1607.01892> 3, 16

Van Wieringen, W. N. and Peeters, C. F. (2016). “Ridge estimation of inverse covariance matrices from high-dimensional data.” *Computational Statistics and Data Analysis*, 103: 284–303.
 URL <http://dx.doi.org/10.1016/j.csda.2016.05.012> 2

Vehtari, A., Gelman, A., and Gabry, J. (2016). “Practical Bayesian model evaluation using leave-one-out cross-validation and WAIC.” *Statistics and Computing*, 27(5): 1–20. 6

Wang, H. (2012). “Bayesian graphical lasso models and efficient posterior computation.” *Bayesian Analysis*, 7(4): 867–886.
 URL https://projecteuclid.org/download/pdfview_1/euclid.ba/1354024465 2, 3

Wang, Z. (2016). “Transactivation of epidermal growth factor receptor by g protein-coupled receptors: Recent progress, challenges and future research.”
 URL <http://www.ncbi.nlm.nih.gov/pubmed/26771606> <http://www.ncbi.nlm.nih.gov/entrez/fcgi?artid=PMC4730337> 1

Won, J.-h., Lim, J., and Kim, S.-J. (2009). “Maximum Likelihood Covariance Estimation.” *Asilomar Conference on Signals, Systems, and Computers*, 1445–1449.
 URL <https://pdfs.semanticscholar.org/f82b/c8eb44f5714a1ffcb8ab25aec401c5ca43c0.pdf> 2

Wong, B. F., Carter, C. K., and Kohn, R. (2003). “Efficient estimation of covariance selection models.” *Biometrika*, 90(4): 809–830. 2

Yuan, T. and Wang, J. (2013). “A coordinate descent algorithm for sparse positive definite matrix estimation.” *Statistical Analysis and Data Mining*, 6(5): n/a–n/a.
 URL <http://doi.wiley.com/10.1002/sam.11185> 2